

# Modes of fault reactivation from analogue modeling experiments: implications for the seismotectonics of the southern Adriatic foreland (Italy)

## Extended abstract

Daniela Di Bucci<sup>a\*</sup>, Antonio Ravaglia<sup>b, c</sup>, Silvio Seno<sup>b</sup>, Giovanni Toscani<sup>b</sup>, Umberto Fracassi<sup>d</sup>, Gianluca Valensise<sup>d</sup>

<sup>a</sup> *Dipartimento della Protezione Civile, Servizio Sismico Nazionale. Via Vitorchiano, 4 - 00189 Roma, Italy*

<sup>b</sup> *Dipartimento di Scienze della Terra, Università di Pavia. Via Ferrata, 1 - 27100 Pavia, Italy*

<sup>c</sup> *now at Midland Valley Exploration Ltd. 14 Park Circus - G3 6AX Glasgow, UK*

<sup>d</sup> *Istituto Nazionale di Geofisica e Vulcanologia, Via di Vigna Murata, 605 - 00143 Roma, Italy*

## \* Corresponding Author:

Daniela Di Bucci  
Dipartimento della Protezione Civile  
Servizio Sismico Nazionale  
Via Vitorchiano, 4  
00189 - Roma, Italy  
Tel.: ++39-06-68204761  
Fax: ++39-06-68202877  
e-mail: [daniela.dibucci@protezionecivile.it](mailto:daniela.dibucci@protezionecivile.it)

**Running title:** Shear zone reactivation: analogue modeling

**Keywords:** Active fault, strike-slip kinematics, fault reactivation, sandbox model.

**Abstract:** The active tectonics at the front of the Southern Apennines and in the Adriatic foreland is characterized by E-W striking, right-lateral seismogenic faults, interpreted as reactivated inherited discontinuities. The best studied among these is the Molise-Gondola shear zone (MGsz). The interaction of these shear zones with the Apennines chain is not yet clear. To address this open question we developed a set of scaled analogue experiments, aimed at analyzing: 1) how dextral strike-slip motion along a pre-existing zone of weakness within the foreland propagates toward the surface and affects the orogenic wedge; 2) the propagation of deformation as a function of increasing displacement; 3) any insights on the active tectonics of Southern Italy. Our results stress the primary role played by these inherited structures when reactivated, and confirm that regional E-W dextral shear zones are a plausible way of explaining the seismotectonic setting of the external areas of the Southern Apennines.

## 1. Introduction

This extended abstract summarizes the main results of a study presented during the 14<sup>th</sup> Meeting of the Association of European Geological Societies (MAEGS14, 2005) and published on *Tectonics* (Di Bucci et al., 2006). The reader may refer to this latter paper for analytical details on the methodology and results as well as a more in-depth discussion.

Until just a few years ago the active tectonics of the Italian peninsula was believed to be dominated by SW-NE extension, occurring all along the axis of the Apennines and accounting for large earthquakes generated by NW-SE normal faults (Valensise and Pantosti eds., 2001; Gruppo di Lavoro CPTI, 2004; Montone et al., 2004). However, the 2002 Molise earthquakes, located to the NE of the Southern Apennines (Fig. 1), supplied evidence that in this part of the chain, toward the foreland, NW-SE normal faulting gives way to E-W, right-lateral, seismogenic faults (e.g. Vallée and Di Luccio, 2005). The inception and growth of these faults date back to Mesozoic times (De Dominicis and Mazzoldi, 1987); therefore, their activity is interpreted as the reactivation of inherited zones of weakness in the present-day tectonic regime, where NW-SE horizontal compression accompanies a SW-NE striking  $\sigma_{\text{hmin}}$  (Montone et al., 2004).

Among the major E-W shear zones (Di Bucci and Mazzoli, 2003; Valensise et al., 2004, and references therein), the best constrained is the Molise-Gondola shear zone (MGsz), which encompasses the source region of the 2002 Molise earthquakes and of the 1627 Gargano earthquake, the Mattinata fault and the Gondola line off-shore (Vallée and Di Luccio, 2005; Patacca and Scandone, 2004a; Tondi et al., 2005; Ridente and Trincardi, 2006, all with references; Fig. 1, Tab. 1). The present-day reactivation of parts of this fault system has been recently constrained by new data from field geology (Mattinata fault; Tondi et al., 2005; Piccardi, 2005) and from very high resolution seismic lines (Gondola line; Ridente and Trincardi, 2006), which show faults displacing Late Pleistocene, Early and Late Holocene deposits.

In this general perspective of fault reactivation, we developed and analyzed a set of sandbox models, aimed at:

- 1) investigating how dextral strike-slip motion along a pre-existing zone of weakness within the foreland, both exposed at the surface and buried below the outer front of the Apennines orogenic wedge, propagates toward the surface and affects the wedge itself;
- 2) analyzing the propagation of deformation from this inherited structure as a function of increasing displacement;
- 3) discussing any insights analogue modeling may supply on the active tectonics and seismogenesis along regional E-W shear zones in Southern Italy.

## 2. Geological setting

The Apennines fold-and-thrust belt is part of a late Cenozoic accretionary wedge (e.g. Patacca and Scandone, 1989; Fig. 1). In the Southern Apennines, this wedge is formed by east-to-northeast verging thrust sheets which derive from paleogeographic domains of alternating carbonate platforms and pelagic basins (Mostardini and Merlini, 1986). The most external of these domains is represented by the Apulia Platform (Fig. 1), that consists of ~ 6 km-thick, shallow-water, Mesozoic carbonates (Ricchetti et al., 1988; Ciaranfi et al., 1988). The deepest ~ 1000 m of this succession are made up of Triassic anhydrite-dolomite deposits (Butler et al., 2004), in turn underlain by fluvial-deltaic Permo-Triassic deposits (Bosellini et al., 1993; Butler et al., 2004) and by an igneous/metamorphic Paleozoic basement (Chiappini et al., 2000; Tiberti et al., 2005).

The Apulia Platform and underlying basement are partly involved in the orogenic wedge, partly form the foreland inflected below the outer front of the Apennines chain and partly form the Adriatic foreland s.s., both on-shore (Gargano and Puglia) and off-shore (Southern Adriatic Sea; Fig. 1). Southern Apennines thrusting progressed toward the Adriatic foreland up to the beginning of the Middle Pleistocene, when the motion of the wedge front ceased (Patacca and Scandone, 2004b). Indeed, a geodynamic change occurred around 800 ka, when SW-NE extension became dominant over the core of the Apennines (Cinque et al., 1993; Galadini, 1999; D'Agostino et al., 2001). As stated in section 1, this tectonic regime is still active; however, areas NE of the Apennine axis display a regime where a NW-SE horizontal compression accompanies a SW-NE striking  $\sigma_{\text{hmin}}$  (Montone et al., 2004). This is demonstrated by the focal mechanisms available for this area, that frequently exhibit N-S and E-W nodal planes and transcurrent kinematics, compatible with a NW-SE striking  $\sigma_{\text{hmax}}$  (e.g., Pondrelli et al., 2006).

The MGsz (Fig. 1) appears as a ~ 15 km-wide and ~ 180 km-long corridor from the Adriatic foreland off-shore to the core of the Apennines. The structural features which compose this shear zone are described in Tab. 1. Whether and how the MGsz continues toward the west of the 2002 Molise earthquakes area is not known. A possible interpretative key is provided by the 1990 Potenza seismic sequence, that occurred on a parallel shear zone more to the south (location on Fig. 1; mainshock on a right-lateral E-W striking plane; aftershocks distributed along the same direction; depth range 14-25 km, i.e. within the basement underlying the Apulia Platform; Di Luccio et al., 2005). This sequence occurred in the most internal buried foreland, where it deepens below the deepest part of the Apennine chain (Menardi Noguera and Rea, 2000). This implies that inherited E-W shear zones could be active at least as far as the buried Adriatic foreland is not involved in thrusting. Similarly, the MGsz could extend for at least 10-15 km west of the 2002 Molise

earthquakes epicentral zone. Hypotheses about a possible continuation of the MGsz further to the west, where the Adriatic foreland is disrupted by thrusting, remain in need of further investigations.

### **3. Experimental set-up**

Sandbox models are a simplified reproduction of the foreland hosting the MGsz and of the overlying outer front of the Apennines orogenic wedge (foredeep deposits included). Scaling (1:200,000) and geological references for the models are summarized in Tab. 2. The experimental apparatus was provided with a right-lateral baseplate fault.

Five sand models were prepared. The first one (SS02, Tab. 3) reproduces a typical wrench zone as classically described in literature (Wilcox et al., 1973; Sylvester, 1988; Mandl, 2000; Le Guerroué and Cobbold, 2006) and was used as a reference for four additional models specifically designed for the present study (SS03 to SS06, Tab. 3). These four models present a layer of glass microbeads within the foreland and at the interface between buried foreland and wedge (Fig. 2 and Tab. 2). Glass microbeads enable low basal friction detachment and inter-strata slip to occur (Sassi et al., 1993; Turrini et al., 2001). The foreland-side of the models, including the part below the wedge, has a vertical discontinuity obtained through a cut that reorganizes the grain distribution, whereas no discontinuity exists on the chain-side and in the wedge itself (Fig. 2). The slightly larger thickness of the chain-side accounts for topography. Displacement on the baseplate fault is progressively larger from one model to another; minimum and maximum displacement values were taken from literature, the other two were chosen as intermediate steps (Tabs. 2 and 3).

Summing up, the experimental set-up identifies three regional-scale domains, east to west (Fig. 2):

- foreland domain **A** = the Adriatic foreland;
- wedge domain **B** = the outer front of the Apennines orogenic wedge and the underlying buried foreland;
- chain domain **C** = the core of the Apennine fold-and-thrust belt.

In the following, we will refer to these domains simply as **A**, **B**, **C**.

### **4. Experimental results**

#### *4.1. Deformation kinematics*

Reference model SS02 (Fig. 3a-h) is compared to model SS03 (Fig. 3i-s), which has the same final displacement of 8.0 cm and includes all the deformation steps of the other experiments.

In SS02, the first fault formed in the western open side of the apparatus, whereas only smooth grid deformation occurred all along the surface (Fig. 3b). After  $D = 1.5$  cm, synthetic Riedel faults developed near the baseplate fault at the two open sides of the box. At  $D = 3.0$  cm, a swarm of en échelon, left-stepped faults appeared diffusely on the entire surface of the model, with faults forming astride the baseplate fault (Fig. 3e). At  $D = 4.5$  cm, P shears sensu Tchalenko (1970) developed between the Riedel faults without cutting them. At the same time, the external branches of the Riedel faults deactivated. At  $D = 5.5$  cm (Fig. 3g), only the faults closest and sub-parallel to the baseplate fault were active. No new faults formed in the final 2.5 cm of basal displacement, the deformation being almost completely accommodated by the same faults (Fig. 3h).

In SS03, the pre-existing cut in the foreland domain **A** immediately transferred the applied displacement up to the surface (Fig. 3m, fault P). The deformation propagated through the wedge front (domain **B**) and the first fault started to form. Grid lines were distorted almost everywhere. After  $D = 1.5$  cm, two faults branched from fault P with a curved shape, both in the receding side of the model only (Fig. 3n). Toward the western open side of the model, faults formed with sinusoidal shape. At  $D = 2.0$  cm, synthetic Riedel faults started to form (Fig. 3o). At  $D = 4.5$  cm, faults formed close to the surface projection of the baseplate fault (Fig. 3q); subsequently, they joined one another and with fault P ( $D = 5.5$ , Fig. 5r). No new faults were observed during the following steps and almost all the deformation was accommodated by the longest E-W fault in the middle of the model. Also in this case the deformation kinematics achieved a steady-state for a displacement of  $\sim 5.5$  cm.

#### *4.2. Deformation geometries*

We focus in particular on model SS06 (final  $D = 0.5$  cm; Figs. 3m and n, and 4), that resulted the most suitable to interpret the MGsz. In domain **A**, displacement was exclusively accommodated by the pre-existing discontinuity P. Fault P offset the wedge front and propagated into domain **B** with a clear bend-off towards the receding half, as expected from the stress change induced at the tip of a strike-slip fault (Mandl, 2000, Lopes Cardozo et al., 2002, Kim et al., 2004). Toward the chain, the distorted grid lines were the only evidence of diffuse deformation. In cross section, fault planes were largely inferred as the layers do not appear clearly displaced and the faults seemed to accommodate only strike-slip activity. Only the contemporaneous view of the surface and of the entire set of sections allowed these subtle faults to be detected. Sections cut in domain **B** show that both fault splays branched at the upper tip of the pre-existing fault P. They became deeper and more steeply dipping as the P tip deepens. At this step of deformation, the vertical throw is either unresolvable or does not exist at all.

In model SS05 (Fig. 5, final  $D = 3.0$  cm), the fault pattern was much more complicated with respect to the previous model. In domain **A**, displacement was again accommodated by fault P without any vertical throw. Within domain **B**, faults affected the receding half of the model and rooted close to the upper tip of fault P forming an asymmetric flower structure, with both reverse and normal vertical throw. In all models, the normal component of motion is seen only in the deeper portion of the fault planes in domain **B**. In domain **C**, faults were present astride and rooted in the baseplate fault, and had reverse component of motion. They formed a symmetric flower structure with topographic uplift of  $\sim 0.5$  cm.

For model SS04 (Fig. 5, final  $D = 5.5$  cm), at the end of the experiment the linkage of fault P with the faults still active resulted in a continuous dextral strike-slip fault that separated completely the two halves of the model. Again, in domain **B** the fault pattern was asymmetrical and developed only in the northern block. The normal component of throw was quite evident for all faults, but was more developed in the high-angle ones. In domain **C**, faults with reverse component of motion developed as a symmetric flower structure (topographic uplift of  $\sim 0.8$  cm).

Finally, in model SS03 (Fig. 5, final  $D = 8.0$  cm) the fault pattern was similar to that of SS04. Actually, no new faults formed during the final 2.5 cm of displacement, and the continuous E-W fault formed by the linkage of the active faults accommodated the whole deformation. In domain **C** the topographic uplift exceeded 1.0 cm.

## **5. Discussion**

### *5.1. Models analysis*

With respect to model SS02, the deformation kinematics of models SS03 to SS06 appears strongly modified by the pre-existing cut. This acted always as a preferential slip surface in domain **A**, thus accommodating the basal displacement since the very first stages of deformation and preventing the inception of any new structures. The presence of the layer of glass microbeads within the sand had no effects, regardless of the amount of displacement.

Toward domain **B**, slip on the pre-existing cut propagated only in the receding block, producing distortion of the grid lines, precursor of the development of faults. Qualitatively, this behavior can be easily understood, since the material is compressed on the advancing side of the fault and stretched on the receding side (Mandl, 2000). To the south of fault P, grid lines remained almost undeformed.

In domain **C**, faults seem to propagate upward into the chain from the baseplate fault, whereas in domain **B** they branch from the upper tip of the pre-existing fault. Therefore, the buried

pre-existing cut acts as an effective baseplate fault just below the wedge, and its immediate activation furthers an early inception of faults in the receding half of domain **B**. Moreover, as the thickness of the overburden chain increases from east to west, the influence of the pre-existing cut diminishes toward the chain. Accordingly, the shear zone width measured at the surface increases toward the west (compare domains **B** and **C** in Fig. 3q-s).

In domain **C**, that had no pre-existing discontinuity, the baseplate fault controlled completely the structural style of the overburden, and the shear zone attained its maximum width where the overlying sand pack is thickest (Tchalenko, 1970; Schöpfer and Steyrer, 2001). Moreover, grid lines started to be greatly deformed long before faults reached the surface.

## *5.2. Insights on the seismotectonics of Southern Apennines*

Our models provide a new interpretative key for the MGsz (compare Figs. 4 and 6). For instance, concerning the present-day activity of the Mattinata fault (Fig. 1, Tab. 1), the chances that this structure is fully reactivated up to the surface are confirmed also for minimal displacement values (Figs. 3m, 4 and 6).

The 1627 Gargano earthquake (Imax X, Mw 6.73; Gruppo di Lavoro CPTI, 2004) caused widespread destruction, more of 5000 victims and a tsunami (Boschi et al., 2000). The epicenter obtained from the damage field is located on shore, between the epicentral area of the 2002 Molise earthquakes and the Gargano promontory, in correspondence with the Apricena fault (Fig. 1). This fault was hypothesized as the source of the 1627 Gargano earthquake by Patacca and Scandone (2004a; Figs. 1, and 6). According to these investigators, it is a 30 km-long, WNW-striking, SSW-dipping normal fault, cutting the whole Quaternary sequence in response to SW-NE large-scale extension. They interpret this fault as a primary structure, whereas dextral strike-slip faults (e.g., Mattinata or the 2002 Molise earthquakes sources) are seen as transfers between large normal faults, i.e., secondary structures. Our experiments suggest that the Apricena fault could be interpreted as one of the splay faults developing within the foredeep at the front of the orogenic wedge from the deeper, pre-existing discontinuity in domain **B** of our models (Fig. 4). Recall that these splays (Figs. 6, 7 and 11) are WNW-striking, SSW-dipping, exhibit a normal component of slip, and form also for relatively low displacements. Moreover, where these splays start deflecting from the direction of the shear zone, no structures are seen at shallow depth above the deep discontinuity (Figs. 3n, 3o and 4). This could explain the state of inactivity of the faults bounding the Chieuti high, as described by Patacca and Scandone (2004a). In summary, the Apricena fault is fully compatible with the hypothesis of it playing a subsidiary role within the MGsz, which is instead the primary structure.

The 2002 Molise earthquakes (Fig. 1) were generated by steeply dipping, right-lateral strike-slip faults, having a cumulative length of  $\sim 15$  km and extending from  $\sim 6$  to 20 km depth (Vallée and Di Luccio, 2005). On the other hand, GPS data revealed limited but well-detectable coseismic deformation at the surface (Giuliani et al., in press). Accordingly, experiments show that in the portion of domain **B** equivalent to the structural setting of the 2002 Molise earthquakes, the pre-existing fault does not reach directly the models' surface until displacement exceeds  $\sim 5$  cm ( $\sim 10$  km in nature). However, also in case of smaller displacements, the models' surface is affected by a ribbon of diffuse strain (Fig. 4, s48).

From a more general perspective, the comparison between our models and the structural setting of the study area further highlights that the complex fault pattern developed for high displacements does not find an obvious equivalent in the modeled part of the Apennines. This favors the hypothesis that the most recent and present-day activity of the MGsz has not yet accumulated a significant displacement. In particular, modeling suggests that cumulative displacements should fall in the 1-6 km range, but more likely closer to the lower bound. This corresponds to a slip rate value quite close to 1.3 mm/a, assuming the present-day tectonic regime as acting since the Middle Pleistocene (about 1 km in 800 ka). This value is comparable to the geological slip rates available in literature (Tabs. 1 and 2).

Finally, we can speculate on the style of possible active structures located west of the 2002 Molise earthquakes (Figs. 1 and 6), and consider displacement values like those discussed above (Fig. 4). In the corresponding models, the pre-existing fault is accompanied by moderately- to steeply-dipping oblique new faults that may or may not reach the surface depending on the horizontal offset. No surface faulting occurs for displacement values corresponding to  $\sim 1$  km in the real world (Fig. 4).

To conclude, we remark that this short note on the modes of fault reactivation is based on analogue models obviously and necessarily simplified. This implies that complexities unaccounted for by the models may exist in the real geological case. Nevertheless, the experiments described (i) provide an independent and innovative tool for addressing an outstanding issue in Italian active tectonics, (ii) outline how relevant is the reactivation of inherited faults in the foreland and at the front of a fold-and-thrust belt, and (iii) confirm that regional E-W trending, dextral shear zones can play a fundamental albeit “hidden” role in the seismotectonic setting of Southern Italy.

**Acknowledgments.** Thanks are due to the MAEGS14 Scientific Committee, who allowed us to present our work in form of extended abstract, and to the Editor and anonymous Reviewers for their comments. Work financially supported by INGV and by PRIN 2004 grant (University of Pavia).



## References

- Aiello, G., De Alteriis, G., 1991. Il margine Adriatico della Puglia: fisiografia ed evoluzione terziaria. *Mem. Soc. Geol. It.* 47, 197-212.
- Anzidei, M., Baldi, P., Casula, G., Crespi, M., Riguzzi, F., 1996. Repeated GPS survey across the Ionian Sea: evidence of crustal deformations. *Geophys. J. Int.* 127, 257-267.
- Argnani, A., Favali, P., Frugoni, F., Gasperini, M., Ligi, M., Marani, M., Mattiotti, G., Mele, G., 1993. Foreland deformational pattern in the Southern Adriatic Sea. *Annali di Geofisica* 36 (2), 229-247.
- Billi, A., 2003. Solution slip and separations on strike-slip fault zones: theory and application to the Mattinata Fault, Italy. *Journal of Structural Geology* 25, 703-715.
- Billi, A., Salvini, F., 2000. Sistemi di fratture associati a faglie in rocce carbonatiche: nuovi dati sull'evoluzione tettonica del Promontorio del Gargano. *Boll. Soc. Geol. It.* 119, 237-250.
- Borre, K., Cacon, S., Cello, G., Kontny, B., Kostak, B., Likke Andersen, H., Moratti, G., Piccardi, L., Stemberk, J., Tondi, E., Vilimek, V., 2003. The COST project in Italy: analysis and monitoring of seismogenic faults in the Gargano and Norcia areas (central southern Apennines, Italy). *Journal of Geodynamics* 36, 3-18.
- Boschi, E., Guidoboni, E., Ferrari, G., Mariotti, D., Valensise, G., Gasperini, P., eds., 2000. Catalogue of strong Italian earthquakes from 461 B.C. to 1997. *Ann. Geophys.* 43, with CD-Rom, 259 p.
- Bosellini, A., Neri, C., Luciani, V., 1993. Guida ai carbonati cretaceo-eocenici di scarpata e bacino del Gargano (Italia meridionale). *Annali dell'Università di Ferrara (Nuova serie), Sezione: Scienze della Terra; vol. 4, Supplemento*, 77 p.
- Butler, R. W. H., Mazzoli, S., Corrado, S., De Donatis, M., Scrocca, D., Di Bucci, D., Gambini, R., Naso, G., Nicolai, C., Shiner, P., Zucconi, V., 2004. Applying thick-skinned tectonic models to the Apennine thrust belt of Italy - Limitations and implications. In: McClay, K., ed., *Thrust tectonics and hydrocarbon systems*. *Am. Ass. Petr. Geol. Memoir* 82, 647-667.
- Casero, P., Roure, F., Endignoux, L., Moretti, I., Muller, C., Sage, L., Vially, R., 1988. Neogene geodynamic evolution of the southern Apennines. *Mem. Soc. Geol. It.* 41, 109-120.
- Casero, P., Roure, F., Vially, R., 1991. Tectonic framework and petroleum potential of the southern Apennines. In: Spencer, A. M., ed., *Generation, Accumulation, and Production of Europe's Hydrocarbons*. *EAPG Special Publication* 1, 381-387.
- Casnedi, R., Moruzzi, G., 1978. Geologia del campo gassifero di Chieuti (Foggia). *Boll. Soc. Geol. It.* 97, 189-196.

- Castello, B., Selvaggi, G., Chiarabba, C., Amato, A., 2005. CSI Catalogo della sismicità italiana 1981-2002, versione 1.0. INGV-CNT, Roma <http://www.ingv.it/CSI/>
- Chiappini, M., Meloni, A., Boschi, E., Faggioni, O., Beverini, N., Carmisciano, C., Marson I., 2000. Shaded relief magnetic anomaly map of Italy and surrounding marine areas. *Annals of Geophysics* 43 (5), 983-989.
- Chilovi C., De Feyter, A. J., Pompucci, A., 2000. Wrench zone reactivation in the Adriatic Block: the example of the Mattinata Fault System (SE Italy). *Boll. Soc. Geol. It.* 119 (1), 3-8.
- Ciaranfi, N., Pieri, P., Ricchetti, G., 1988. Note alla carta geologica delle Murge e del Salento (Puglia centromeridionale). *Mem. Soc. Geol. It.* 41, 449-460.
- Cinque, A., Patacca, E., Scandone, P., Tozzi, M., 1993. Quaternary kinematic evolution of the southern Apennines. Relationship between surface geological features and deep lithospheric structures. *Annali di Geofisica* 36, (2), 249-260.
- Colantoni, P., Tramontana, M., Tedeschi, R., 1990. Contributo alla conoscenza dell'avampaese apulo: struttura del Golfo di Manfredonia (Adriatico meridionale). *Giornale di Geologia, serie 3a*, 52 (1-2), 19-32.
- D'Agostino, N., Jackson, J. A., Dramis, F., Funicello, R., 2001. Interactions between mantle upwelling, drainage evolution and active normal faulting: an example from the central Apennines (Italy). *Geophysical Journal International* 147, 475-497.
- de Alteriis, G., 1995. Different foreland basins in Italy: examples from the central and southern Adriatic Sea. *Tectonophysics* 252, 349-373.
- De' Dominicis, A., Mazzoldi, G., 1987. Interpretazione geologico-strutturale del margine orientale della Piattaforma apula. *Mem. Soc. Geol. It.* 38, 163-176.
- Di Bucci, D., S. Mazzoli, 2003. The October-November 2002 Molise seismic sequence (southern Italy): an expression of Adria intraplate deformation. *J. Geol. Soc. London* 160 (4), 503-506.
- Di Bucci, D., Ravaglia, A., Seno, S., Toscani, G., Fracassi, U., Valensise, G., 2006. Seismotectonics of the Southern Apennines and Adriatic foreland: insights on active regional E-W shear zones from analogue modeling. *Tectonics* 25, TC4015, doi:10.1029/2005TC001898.
- Di Luccio, F., Piscini, A., Pino, N. A., Ventura, G., 2005. Reactivation of deep faults beneath Southern Apennines: evidence from the 1990–1991 Potenza seismic sequences. *Terra Nova* 00, 1-5.
- Ferranti, L., Oldow, J., 2005. Latest Miocene to Quaternary horizontal and vertical displacement rates during simultaneous contraction and extension in the Southern Apennines orogen, Italy. *Terra Nova* 17, 209-214.

- Finetti, I., 1982. Structure, stratigraphy and evolution of the Central Mediterranean. *Boll. Geofis. Teor. Appl.* 24, 247-312.
- Funiciello, R., Montone, P., Salvini, F., Tozzi, M., 1988. Caratteri strutturali del Promontorio del Gargano. *Mem. Soc. Geol. It.* 41, 1235-1243.
- Galadini, F., 1999. Pleistocene changes in the central Apennine fault kinematics: A key to decipher active tectonics in central Italy. *Tectonics* 18 (5), 877-894.
- Giuliani, R., Anzidei, M., Bonci, L., Calcaterra, S., D'Agostino, N., Mattone, M., Pietrantonio, G., Riguzzi, F., Selvaggi, G., in press. Co-seismic displacements associated to the Molise (Southern Italy) earthquake sequence of October-November 2002 inferred from GPS measurements. *Tectonophysics*.
- Gruppo di Lavoro CPTI, 2004. Catalogo Parametrico dei Terremoti Italiani, versione 2004 (CPTI04). INGV, Bologna, <http://emidius.mi.ingv.it/CPTI/>
- Kim, Y.-S., Peacock, D. C. P., Sanderson, D. J., 2004. Fault damage zones. *Journal of Structural Geology* 26, 503-517.
- Le Guerroué, E., Cobbold, P. R., 2006. Influence of erosion and sedimentation on strike-slip fault systems: insights from analogue models. *Journal of Structural Geology* 28, 421–430.
- Lopes Cardozo, G., Bada, G., Lankreijer, A., Nieuwland, D., 2002. Analogue modeling of a prograding strike-slip fault: case study of the Balatonfo fault, western Hungary. *EGU Stephan Mueller Special Publication Series* 3, 217-226.
- Mandl, G., 2000. *Faulting in Brittle Rocks*, 434 pp., Springer, Berlin.
- Menardi Noguera, A., Rea, G., 2000. Deep structure of the Campanian-Lucanian Arc (southern Apennines). *Tectonophysics* 324, 239-265.
- Montone, P., Mariucci, M. T., Pondrelli, S., Amato, A., 2004. An improved stress map for Italy and surrounding regions (central Mediterranean). *Journal of Geophysical Research* 109 (B10410), 1-22, doi: 10.1029/1003JB002703.
- Morelli, D., 2002. Evoluzione tettonico-stratigrafica del Margine Adriatico compreso tra il Promontorio garganico e Brindisi. *Mem. Soc. Geol. It.* 57, 343-353.
- Mostardini, F., Merlini, S., 1986. Appennino centro-meridionale. *Sezioni Geologiche e Proposta di Modello Strutturale*. *Mem. Soc. Geol. It.* 35, 177-202.
- Patacca, E., Scandone, P., 1989. Post-Tortonian mountain building in the Apennines. The role of the passive sinking of a relic lithospheric slab. In: Boriani, A., M. Bonafede, G. B. Piccardo, and G. B. Vai, eds., *The Lithosphere in Italy*. *Atti dei Convegni Lincei* 80, 157-176.
- Patacca, E., Scandone, P., 2004a. The 1627 Gargano earthquake (Southern Italy): Identification and characterization of the causative fault. *Journal of Seismology* 8 (2), 259-273.

- Patacca, E., Scandone, P., 2004b. The Plio-Pleistocene thrust belt – foredeep system in the Southern Apennines and Sicily (Italy). In: Crescenti, U., S. D’Offizi, S. Merlini, and L. Lacchi, eds., *Geology of Italy*. Società Geologica Italiana, Roma, 232 pp.
- Patacca, E., Scandone, P., Tozzi, M., 2000. Il profilo CROP04. *Protecta* 10-12, 49-52.
- Piccardi, L., 1998. Cinematica attuale, comportamentosismico e sismologia storica della faglia di Monte Sant’Angelo (Gargano, Italia): la possibile rottura superficiale del “leggendario” terremoto del 493 d.C. *Geogr. Fis. Dinam. Quat.* 21, 155-166.
- Piccardi, L., 2005. Paleoseismic evidence of legendary earthquakes: The apparition of Archangel Michael at Monte Sant’Angelo (Italy). *Tectonophysics* 408, 113–128.
- Pondrelli, S., Salimbeni, S., Ekström, G., Morelli, A., Gasperini, P., Vannucci, G., 2006. The Italian CMT dataset from 1977 to the present. *Phys. Earth Planet. Int.* 159 (3-4), 286-303. [doi:10.1016/j.pepi.2006.07.008](https://doi.org/10.1016/j.pepi.2006.07.008)
- Ricchetti, G., Ciaranfi, N., Luperto Sinni, E., Mongelli, F., Pieri, P., 1988. Geodinamica ed evoluzione sedimentaria e tettonica dell’avampaese apulo. *Mem. Soc. Geol. It.* 41, 57-82.
- Ridente, D., Trincardi, F., 2006. Active foreland deformation evidenced by shallow folds and faults affecting late Quaternary shelf-slope deposits (Adriatic Sea, Italy). *Basin Research* 18 (2), 171-188. [doi: 10.1111/j.1365-2117.2006.00289.x](https://doi.org/10.1111/j.1365-2117.2006.00289.x)
- Sassi, W., Colletta, B., Balé, P., Paquereau, T., 1993. Modelling of structural complexity in sedimentary basins: the role of pre-existing faults in thrust tectonics. *Tectonophysics* 226, 97-112.
- Schöpfer, M. P. J., Steyrer, H. P., 2001. Experimental modeling of strike-slip faults and the self-similar behavior. In: Koyi, H. A., Mancktelow, N. S., eds., *Tectonic Modeling: A Volume in Honor of Hans Ramberg*. Geological Society of America Memoir 193, 21-27.
- S.G.N., Servizio Geologico Nazionale, 1965. Carta geologica d'Italia, scale 1:100.000, Sheet 157 "Monte S. Angelo", II edition.
- S.G.N., Servizio Geologico Nazionale, 1970. Carta geologica d'Italia, scale 1:100,000, Sheet 156 "S. Marco in Lamis", II edition.
- Sylvester, A. G., 1988. Strike-slip faults. *Geol. Soc. Am. Bull.* 100, 1666-1703.
- Tchalenko, J. S., 1970. Similarities between shear zones of different magnitudes. *Geol. Soc. Am. Bull.* 81, 1625-1640.
- Tiberti, M. M., Orlando, L., Di Bucci, D., Bernabini, M., Parotto, M., 2005. Regional gravity anomaly map and crustal model of the Central-Southern Apennines (Italy). *Journal of Geodynamics* 40, 73-91.

- Tondi, E., Piccardi L., Cacon S., Kontny B., Cello G., 2005. Structural and time constraints for dextral shear along the seismogenic Mattinata fault (Gargano, southern Italy). *Journal of Geodynamics* 40, 134-152.
- Turrini, C., Ravaglia, A., Perotti, C. R., 2001. Compressional structures in a multilayered mechanical stratigraphy: insights from sandbox modelling with three-dimensional variations in basal geometry and friction. In: Koyi, H. A., Mancktelow, N. S., eds., *Tectonic Modeling: A Volume in Honor of Hans Ramberg*. Geological Society of America Memoir 193, 153-178.
- Valensise, G., Pantosti, D., eds., 2001. Database of Potential Sources for Earthquakes Larger than M 5.5 in Italy. *Annals of Geophysics* 44 (1), with CD-ROM.
- Valensise, G., Pantosti, D., Basili, R., 2004. Seismology and Tectonic Setting of the Molise Earthquake Sequence of October 31-November 1, 2002. *Earthq. Spectra* 20 (1), 23-37.
- Vallée, M., Di Luccio, F., 2005. Source analysis of the 2002 Molise, southern Italy, twin earthquakes (10/31 and 11/01). *Geophysical Research Letters* 32, L12309, 1-4, doi:10.1029/2005GL022687
- Wilcox, R. E., Harding, T. P., Seely, D. R., 1973. Basic wrench tectonics. *The American Association of Petroleum Geologists Bulletin* 57 (1), 74-96.
- Winter, T., Tapponnier, P., 1991. Extension majeure post-Jurassique et ante-Miocène dans le centre de l'Italie: données microtectoniques. *Bull. Soc. Géol. France* 162 (6), 1095-1108.

## Figure and table captions

**Fig. 1.** Geological sketch map of peninsular Italy from the Po Plain to the northern end of the Calabrian arc (after Butler et al., 2004, modified), showing location of the modeled area and the Mattinata-Gondola shear zone (MGsz).

**Fig. 2.** Sketch of the experimental set-up. Two fixed sidewalls parallel to the strike-slip motion confine the sand, whereas the model is open on the other two sides. The three regional-scale domains (**A**, **B**, **C**) are discussed in the text.

**Fig. 3.** Interpreted plan-views of the deformation kinematics of reference model SS02 (left; a-h) and model SS03 (right; i-s). Reference vertical lines are spaced  $\sim 5.5$  cm. The horizontal hatched line is the baseplate fault, BF. In model SS03 (i), the dotted line represents the pre-existing fault P, buried under the front of the Apennine chain. Labels **A**, **B** and **C** mark the three regional-scale domains (see Fig. 2). Final displacement was  $D = 8.0$  cm. The newly formed faults are indicated with an arrow showing the sense of propagation through the sand surface. They strictly refer to the specific step shown (in plan-view, deformation kinematics was analyzed at every 0.5 cm step of basal displacement).

**Fig. 4.** Interpreted map-view and cross sections of model SS06. Final displacement was  $D = 0.5$  cm. In plan view, the E-W dotted line is the surface projection of the baseplate fault, whereas the hatched lines represent faults or part of them that do not reach the surface. P marks the pre-existing fault, both exposed and buried under the front of the Apennine chain. Labels **A**, **B** and **C** indicate the three regional-scale domains (see Fig. 2). In the sections, the two layers of glass microbeads are also indicated.

**Fig. 5.** Examples of deformation in the three regional-scale domains **A**, **B** and **C** for progressively higher displacement values ( $D = 3.0$ ,  $5.5$  and  $8.0$  cm, respectively).

**Fig. 6.** Spots on the MGsz corresponding to Fig. 4 (all taken from literature, modified and redrawn as needed). Three of these geological sections are at regional scale, and the oblique orientation with respect to the sections of the models does not invalidate the observed analogies. Dark grey refers to the chain, the frontal wedge and the foredeep deposits. Light grey refers to the foreland. *a1*, *a2*. Geological sections across the Mattinata fault (S.G.N., 1965; 1970). The well defined setting of the

fault is continuous over its entire length. **b.** Geological section across the Apricena fault and Chieuti high (Patacca and Scandone, 2004a). **c.** Regional section crossing the epicentral area of the 2002 Molise earthquakes (Mostardini and Merlini, 1986). **d.** Regional section across the westernmost part of the study area (Butler et al., 2004). The projection of the 2002 Molise sequence focal volume is highlighted by the dashed ellipse.

-----

**Tab.1.** Details and references on the MGsz.

**Tab. 2.** Scaling of the models (1:200,000) vs. geological parameters.

**Tab. 3.** List of the experiments described in this study and of their geometrical parameters.

**Table 1.**

Structure	Location	Comments	Activity	References
<i>Gondola line</i>	Off-shore Gargano Promontory	Repeatedly reactivated under different tectonic regimes before, during and after the Apennine chain build-up (e.g., Mesozoic extension, Cenozoic shortening), both with right- and left-lateral components of motion.	It affects the sea bottom, suggesting Quaternary activity, but seismic reflection lines allowed its motion to be detected since Cretaceous.	Aiello and de Alteriis, 1991; Argnani et al., 1993; Colantoni et al., 1990; de Alteriis, 1995; De' Dominicis and Mazzoldi, 1987; Morelli, 2002; Patacca and Scandone, 2004a; Ridente and Trincardi, 2006
<i>Mattinata fault</i>	Exposed on the Gargano Promontory	Intensely investigated from a regional, structural and seismotectonic point of view.	A polyphase activity has been recognized, and the complex fault kinematics is still matter of debate. Most investigators agree on a present-day right-lateral main component of motion, as confirmed by the focal mechanisms of the 19 June 1975 and 24 July 2003 earthquakes, GPS data, geomorphological and paleoseismological investigations. Interpreted as the source of historical earthquakes (e.g.: 493 AD, 1875). Instrumental seismicity recorded within the first 25 km of the crust of the Gargano area.	Anzidei et al., 1996; Billi and Salvini, 2000; Billi, 2003; Borre et al., 2003; Castello et al., 2005; Chilovi et al., 2000; Ferranti and Oldow, 2005; Finetti, 1982; Funicello et al., 1988; Piccardi, 1998; Piccardi, 2005; Tondi et al., 2005; Valensise and Pantosti, eds., 2001; Valensise et al., 2004; Winter and Tapponier, 1991
<i>Apricena fault; Chieuti high; 1627 Gargano earthquake source</i>	West of the Gargano Promontory, where the foreland plunges below the Plio-Pleistocene deposits of the recent-most foredeep (Bradanic Trough)	At depth, at the top of the buried Apulia Platform, an E-W ridge is preserved along strike of the Mattinata fault. This structure has been recently interpreted as a push-up related to strike-slip motion. It is accompanied by WNW-ESE striking, SSW dipping faults with a normal component of motion.	The Apricena fault has been interpreted as the seismogenic source of the 1627 Gargano earthquake ( $M_e = 6.8$ ). Scattered clues of recent activity on E-W structures, both in this area and more to the west, are also provided by the drainage pattern, that shows consistent E-W trending anomalies.	Casnedi and Moruzzi, 1978; Patacca and Scandone, 2004a; Gruppo di Lavoro CPTI, 2004; Valensise et al., 2004
<i>2002 Molise earthquakes sources</i>	Where the Apulia Platform and underlying basement deepen below the outer front of the Apennine orogenic wedge	In this area, the buried Apulia Platform is ~ 6 km thick and its top lies at ~ 3000 m depth.	Both the mainshocks of the sequence had similar magnitude ( $M_w = 5.8-5.7$ ), hypocenters at 16 and 18 km, respectively, and almost pure strike-slip focal mechanism, with right-lateral motion on E-W trending nodal planes. The aftershocks distribution also follows an E-W direction, and surface coseismic deformation revealed by GPS data is consistent with this kinematics, but no surface faulting accompanied these earthquakes. Activity mainly took place in a crustal volume between 10 - 24 km depth. The seismogenic structures of the 2002 Molise earthquakes are located essentially within the Paleozoic basement of the Apulia Platform.	Butler et al., 2004; Giuliani et al., in press; Mostardini and Merlini, 1986; Valensise et al., 2004; Vallée and Di Luccio, 2005



**Table 2.**

<b>Analogue models SS03 - SS06</b>	<b>Geological reference</b>
Model length = more than 100 cm	MGsz minimum length = 180 km + 10-15 km
Model width = 50 cm (to avoid lateral effects)	MGsz width = ca. 15 km
Minimum thickness (foreland-side) = 10 cm	Seismogenic layer in the foreland = 20 km
Maximum thickness (orogenic wedge-side) = 11 cm	2000 m of topographic relief are added in the orogenic wedge area = 22 km
Dip angle of the wedge = ca. 20°	After published regional geological cross-sections (Casero et al., 1988; 1991; Patacca et al., 2000; Menardi Noguera and Rea, 2000; Butler et al., 2004)
0.5 cm-thick layer of glass microbeads at 3.5 km depth in the foreland-side of the model	ca. 1000 m thick anhydrite-dolomite deposits at the bottom of the Apulia Platform succession (total thickness = 6000 m)
0.3 cm ca. thick layer of glass microbeads between the wedge and the underlying foreland	It simulates the physical discontinuity between the orogenic wedge and the underlying foreland
Right-lateral baseplate fault, in the middle of the model and perpendicular to the wedge front	Crustal wrench zone with right-lateral sense of motion
Vertical discontinuity = a cut in the foreland-side and below the wedge (that is not cut), made by means of 0.5 mm thick nylon thread located in correspondence with the baseplate fault	MGsz activity dated back to Mesozoic times. The orogenic wedge reached the present-day location in Middle Pleistocene
Minimum right-lateral displacement = 0.5 cm	Horizontal slip rate 1.0 mm/a after Piccardi (1998); 0.7-0.8 mm/a after Tondi et al. (2005); cumulative since Middle Pleistocene = less than 1 km
Maximum right-lateral displacement = 8.0 cm	15 km, after De' Dominicis and Mazzoldi (1987) as interpreted by Chilovi et al. (2000)

**Table 3.**

<b>Experiment</b>	<b>Pre-existing cut</b>	<b>Layer of glass microbeads in the foreland</b>	<b>Presence of the wedge</b>	<b>Thickness</b>	<b>Displacement</b>
SS02	No	No	No	10 cm	8.0 cm
SS03	Yes	Yes	Yes	10-11 cm	8.0 cm
SS04	Yes	Yes	Yes	10-11 cm	5.5 cm
SS05	Yes	Yes	Yes	10-11 cm	3.0 cm
SS06	Yes	Yes	Yes	10-11 cm	0.5 cm



Figure 2  
[Click here to download high resolution image](#)

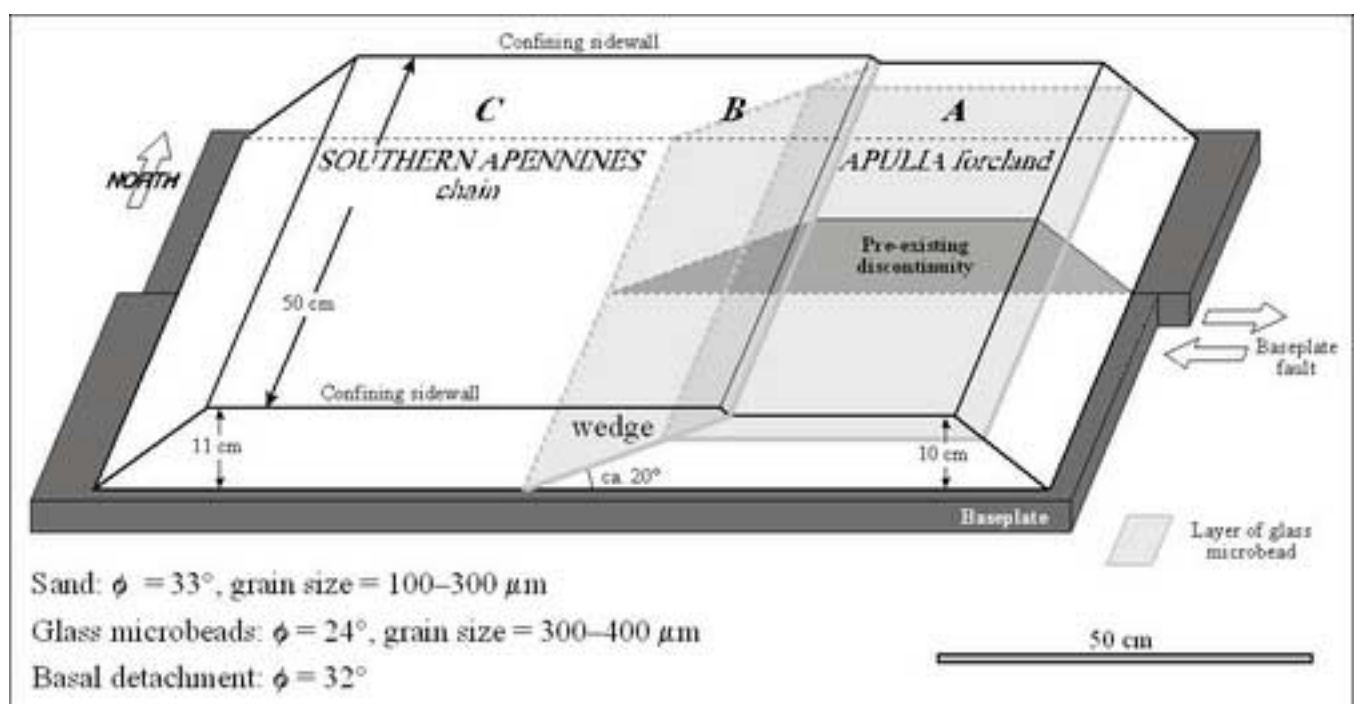


**Figure 3**  
[Click here to download high resolution image](#)

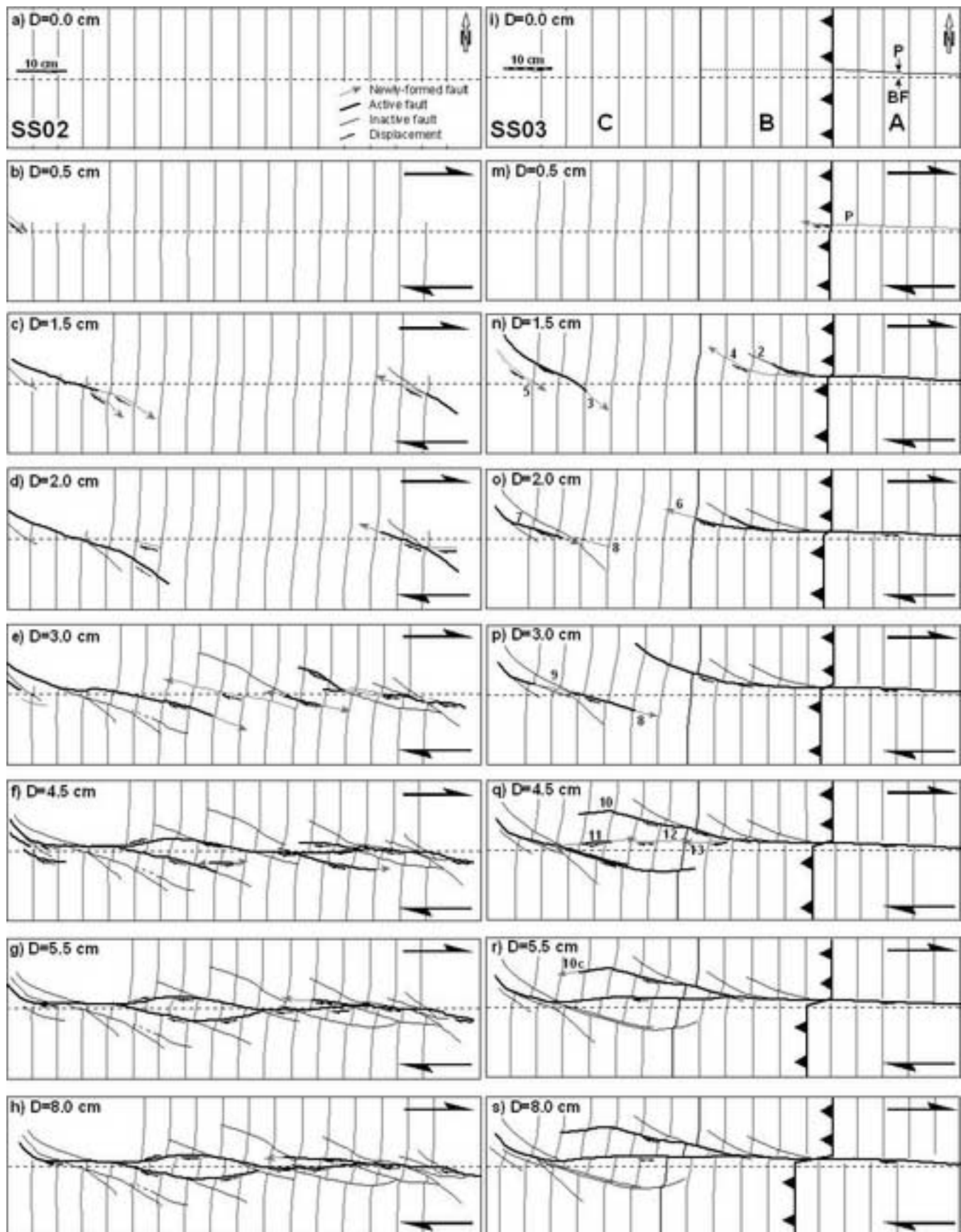


Figure 4  
[Click here to download high resolution image](#)

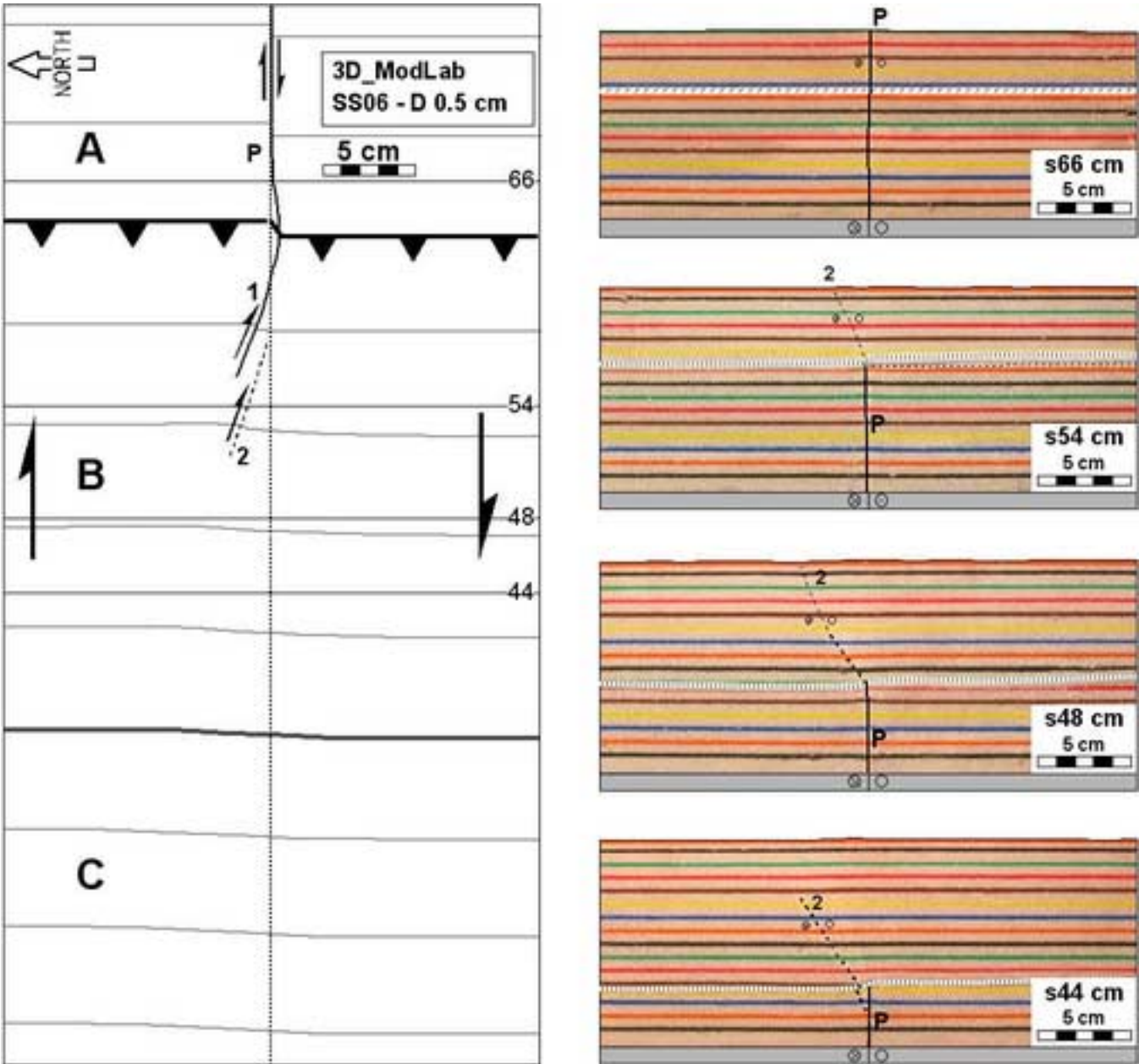


Figure 5  
[Click here to download high resolution image](#)

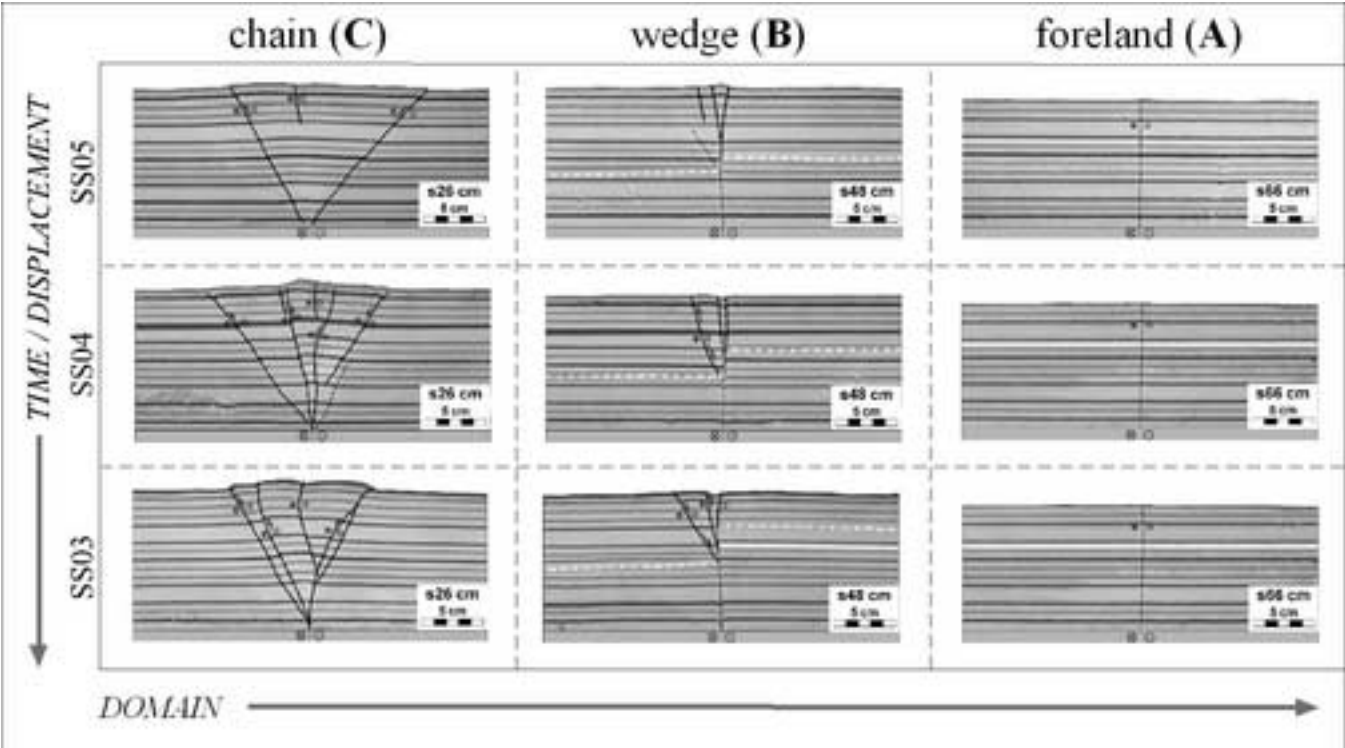




Figure 6  
[Click here to download high resolution image](#)

